Yan, R., Woith, H., Wang, R., Zhang, Y. (2016): Earth's free oscillations excited by the 2011 Tohoku Mw 9.0 earthquake detected with a groundwater level array in mainland China. - *Geophysical Journal International*, *206*, 3, pp. 1457—1466.

DOI: http://doi.org/10.1093/gji/ggw213

Geophysical Journal International

Geophys. J. Int. (2016) **206,** 1457–1466
Advance Access publication 2016 June 8
GJI Seismology

doi: 10.1093/gji/ggw213

Earth's free oscillations excited by the 2011 Tohoku M_w 9.0 earthquake detected with a groundwater level array in mainland China

Rui Yan,[1,2] Heiko Woith,[3] Rongjiang Wang[3] and Yong Zhang[4]

[1]*China Earthquake Networks Center,* 100045 *Beijing, China*
[2]*School of Water Resources and Environment, China University of Geosciences, Beijing* 100083*, China*
[3]*GFZ German Research Centre for Geosciences, D-*14473 *Potsdam, Germany. E-mail: heiko.woith@gfz-potsdam.de*
[4]*School of Earth and Space Sciences, Peking University, Beijing* 100871*, China*

Accepted 2016 June 2. Received 2016 June 1; in original form 2015 September 21

SUMMARY

Earth's free oscillations excited by a mega-thrust earthquake were observed by a continent-scale array of groundwater monitoring sites for the first time. After the occurrence of the 2011 Tohoku M_w 9.0 earthquake, water level records at 43 out of 216 wells in the China mainland revealed long-period free oscillation signals. In the time domain, these free oscillations exhibit globe circling Rayleigh surface waves. In some single wells, even the globe-circling Rayleigh wave R7 was visible, which travels three times around the Earth after the first arrival and appears about 10 hr after the earthquake occurrence in the present case. The spectral analysis shows that the principal oscillatory fluctuations seen in the water level records correspond to the spheroidal modes ${}_0S_l$ ($l = 2$–31 for frequencies between 0.3 and 5.0 mHz) of the Earth's free oscillation. Especially at quiet sites, the spheroidal modes at very low frequencies (<1.5 mHz) can be identified with high signal-to-noise ratios. Using signal enhancement methods (product spectrum over 43 wells), even the gravest modes of these oscillations can be detected. The results suggest that groundwater level arrays can be considered as a low-cost complementary tool to study the Earth's free oscillations excited by great earthquakes. Additionally, the site-specific aquifer response may provide further insight into local hydrogeological conditions.

Key words: Time-series analysis; Hydrogeophysics; Surface waves and free oscillations; Asia.

1 INTRODUCTION

Free oscillations of the Earth have been used to constrain and provide insight into the Earth's deep interior structure and its dynamics (Ness *et al*. 1961; Laske & Masters 1999; Woodhouse & Deuss 2007; Molodenskii & Molodenskaya 2009; Molodenskii 2010), to understand the focal mechanisms of earthquakes (Kanamori & Anderson 1975; Park *et al*. 2005; Lambotte *et al*. 2007; Okal & Stein 2009; Bogiatzis & Ishii 2014) and to recognize slow and silent earthquakes (Beroza & Jordan 1990). Theories of the Earth's free oscillations which have been discussed since the latter part of the 19th century were gradually verified by experimental observations during the late 1950s and 1960s. Originally, only gravimeters and strainmeters were used to monitor the Earth's free oscillations. Benioff (1958) attempted to find free oscillations after a large Kamtchatka earthquake and found oscillations with about the period of ${}_0S_2$ visible in the strain record. Benioff *et al*. (1959) were searching for the incessant free oscillations, but did not find anything, and concluded that their amplitude must be less than 1 μgal. Today we know that they are a factor of 1000 times smaller. Benioff *et al.* (1961) detected normal modes after the great Chilean earthquake. After that, a wide range of normal modes were observed by different kinds of instruments. In particular, both spheroidal and torsional oscillations were revealed by a power spectral analysis of seismograms recorded by different seismographs. Alsop *et al.* (1961) analysed periods of the graver modes of oscillations with a strain seismograph and a pendulum seismograph. Derr (1969) estimated an earth model through least-squares inversion with weighted means of observed periods of free oscillations recorded by spring gravimeters. Dziewonski & Gilbert (1972) made an intensive search for the Earth's eigenperiods with long-period seismographs from the World-Wide Standardized Seismograph Network. Modern seismometers like the STS-1 can detect the longest period normal modes (Deuss *et al*. 2011). Igel *et al.* (2011) and Nader *et al.* (2012) explored observations of the Earth's toroidal free oscillations recorded on a ring laser system, which is sensitive to rotational ground motions around a vertical axis. Ferreira *et al.* (2006) suggested that long-base fluid tube tiltmeters could potentially contribute to obtaining high-quality measurements

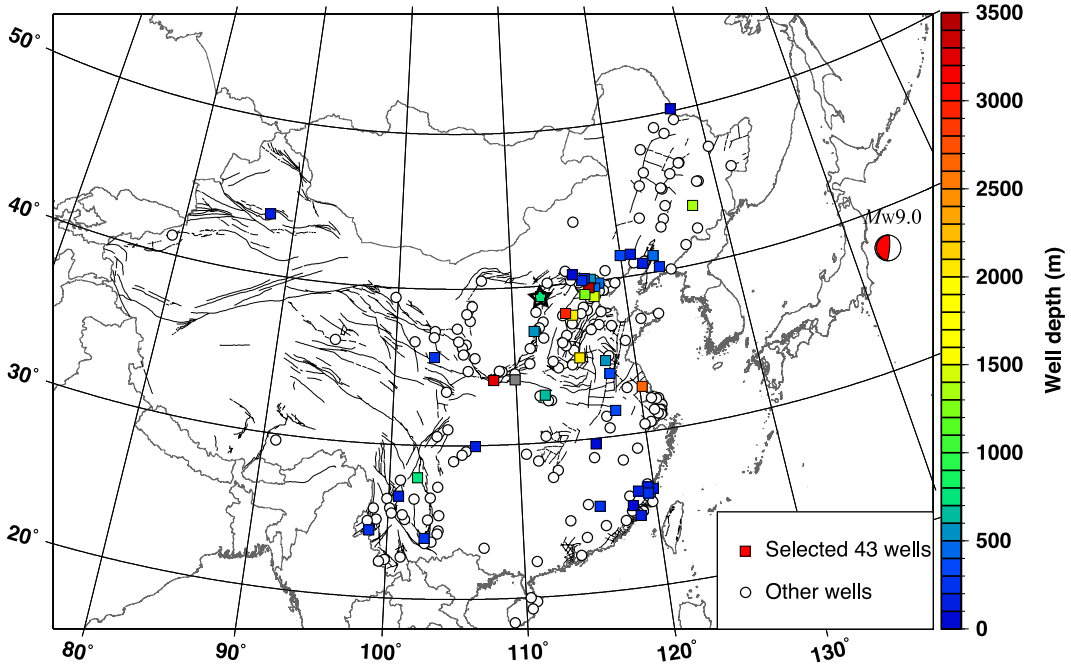

Figure 1. Distribution of 43 selected well sites where the Earth's free oscillations excited by the M_w 9 Tohoku earthquake were recorded. Well depths are indicated by coloured symbols. Squares depict the selected 43 wells. Circles indicate other wells. The star marks the YMG seismic station.

of the long-period seismic surface waves and free oscillations. Park *et al.* (2008) reported long-period toroidal free oscillations from the great Sumatra–Andaman earthquake observed by paired laser extensometers in Gran Sasso, Italy. Recently, Mitsui & Heki (2012) observed Earth's free oscillation excited by the 2011 Tohoku earthquake by a dense GPS array of more than 300 stations in Japan, and Zürn *et al.* (2015) showed high-quality low frequency normal mode strain observations for the 2011 Tohoku earthquake.

A confined well-aquifer system can be viewed as a strain meter. The sensitivity of such a system to strain is associated with the poroelastic and hydraulic properties of the aquifer and the geometry of the boreholes (Bodvarsson 1970). Water level oscillations are usually recorded in wells during the passage of seismic waves caused by large earthquakes. Already in the 1960s it was suggested that major water level oscillations have been induced by long-period surface waves (Eaton & Takasaki 1959; Rexin *et al*. 1962). Cooper *et al.* (1965) formulated analytical solutions relating the amplification to the transmissivity and storage coefficient of the aquifer, the well dimensions and the period of the seismic wave. Liu *et al.* (1989) synthesized the results of previous studies and improved the analytical solution for amplification. Brodsky *et al.* (2003) extended these models and applied them to fractured aquifers. All of these studies were focused on surface waves with periods of several tens of seconds. However, only very few studies exist on longer-period free oscillation signals recorded by groundwater level (Kawabe *et al*. 1988; Ren *et al*. 2009).

In this study, we demonstrate that long-period oscillations excited by the Tohoku M_w 9.0 earthquake were widely observed by water level stations in mainland China. Groundwater level data with a sampling interval of 1 min allow the analysis of Earth's free oscillations. An autoregressive (AR) spectral estimation method was used to detect free oscillation modes in each water level time series, while a simple array analysis of product spectra of time series from 43 well sites was used to improve the signal-to-noise ratios (SNRs). The seismically-induced water level oscillations were then compared with velocity records from broadband seismometer in the major frequency band of the free oscillations. The results show that water level arrays can detect spheroidal modes of the Earth's free oscillations down to very low frequencies.

2 OBSERVATIONS AND DATA

An M_w 9.0 earthquake occurred at 05:46:24 UTC on 2011 March 11 off the Pacific coast of Tohoku, Honshu Island, Japan. The earthquake resulted from mega-thrust faulting on the subduction zone between the Pacific and the Okhotsk plates. The fault rupture extended about 200 km along dip, while the aftershock zone covered a length of about 500 km along strike of the subduction zone. The average slip was about 10 m (Ide *et al*. 2011; Suzuki *et al*. 2011; Kubo & Kakehi 2013; Hwang 2014). This is the largest earthquake ever recorded with modern instruments in Japan and is the fourth largest earthquake recorded instrumentally in the world since 1900 in the historical catalogue.

Following the 2011 Tohoku M_w 9.0 earthquake, groundwater level data from 216 well sites of the Groundwater Monitoring Network of China Earthquake Networks Center were analysed. The well water levels were measured by LN-3A digital piezometer recorders manufactured by the Institute of Earthquake Science, which belongs to the China Earthquake Administration (CEA). The piezometer readings are converted into groundwater level with a resolution of 1 mm over the range between 0 and 10 m; absolute accuracy is 0.2 per cent full scale. The sampling interval of the observation data was one minute, the data logger clock being synchronized with GPS. All the wells are open. Most of the wells were drilled into consolidated rock, mainly limestone, sandstone and magmatic rocks. The boreholes were cased to specific aquifers down to a depth of 5269 m. The diameters of perforated well sections range from 75 to 216 mm. The majority of the aquifers show a high degree of confinement; most of the aquifer systems are sensitive to Earth tides. Phases and

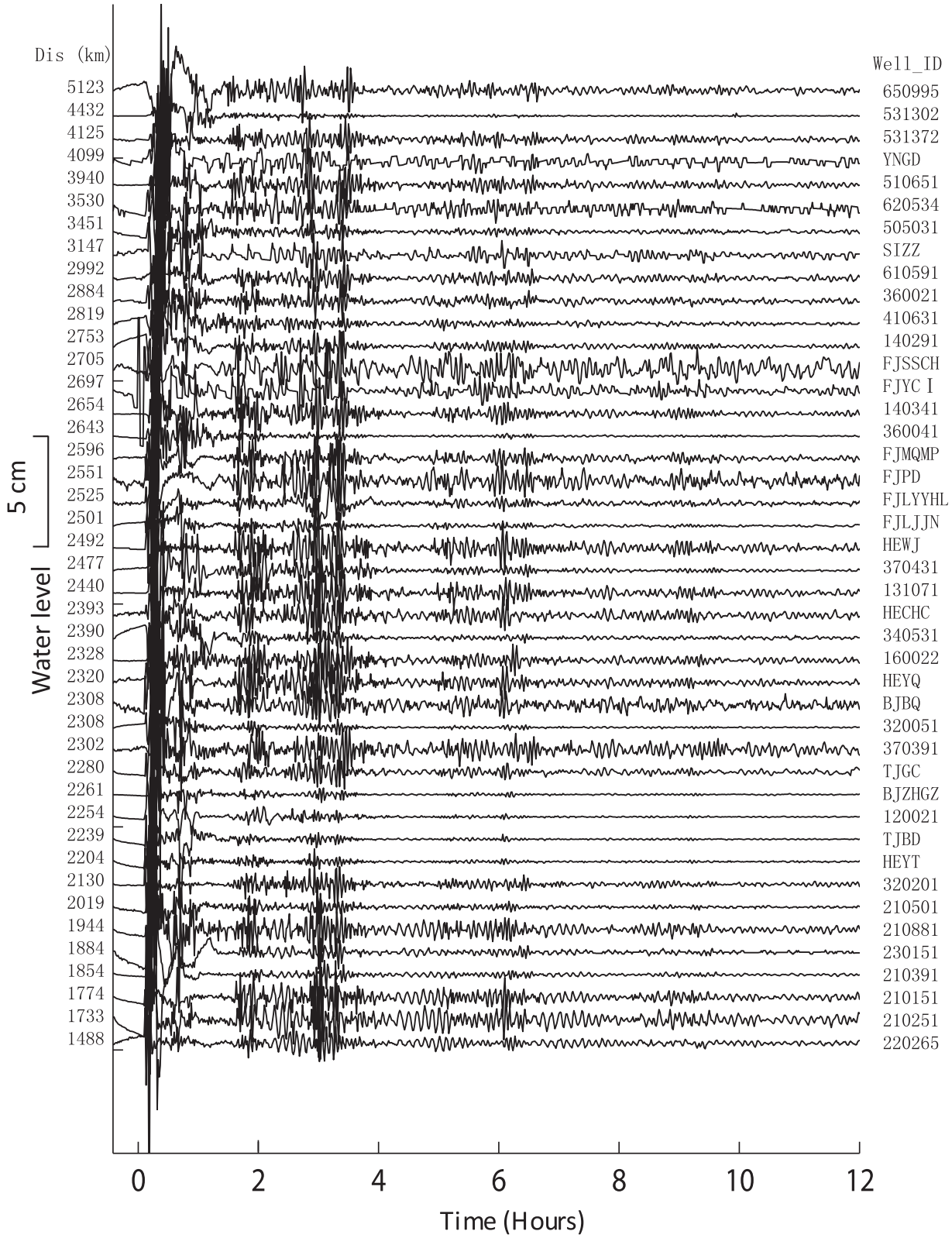

Figure 2. 12 hr data of water level fluctuations after the M_w 9 Tohoku earthquake of 2011 observed at 43 well sites sorted by well-epicentre distances. The data are filtered with periods of 2–64 min by a Daubechies Wavelet (db4) bandpass filter. Zero point of horizontal coordinate corresponds to the origin time of the earthquake. Well IDs are shown on the right side of each curve.

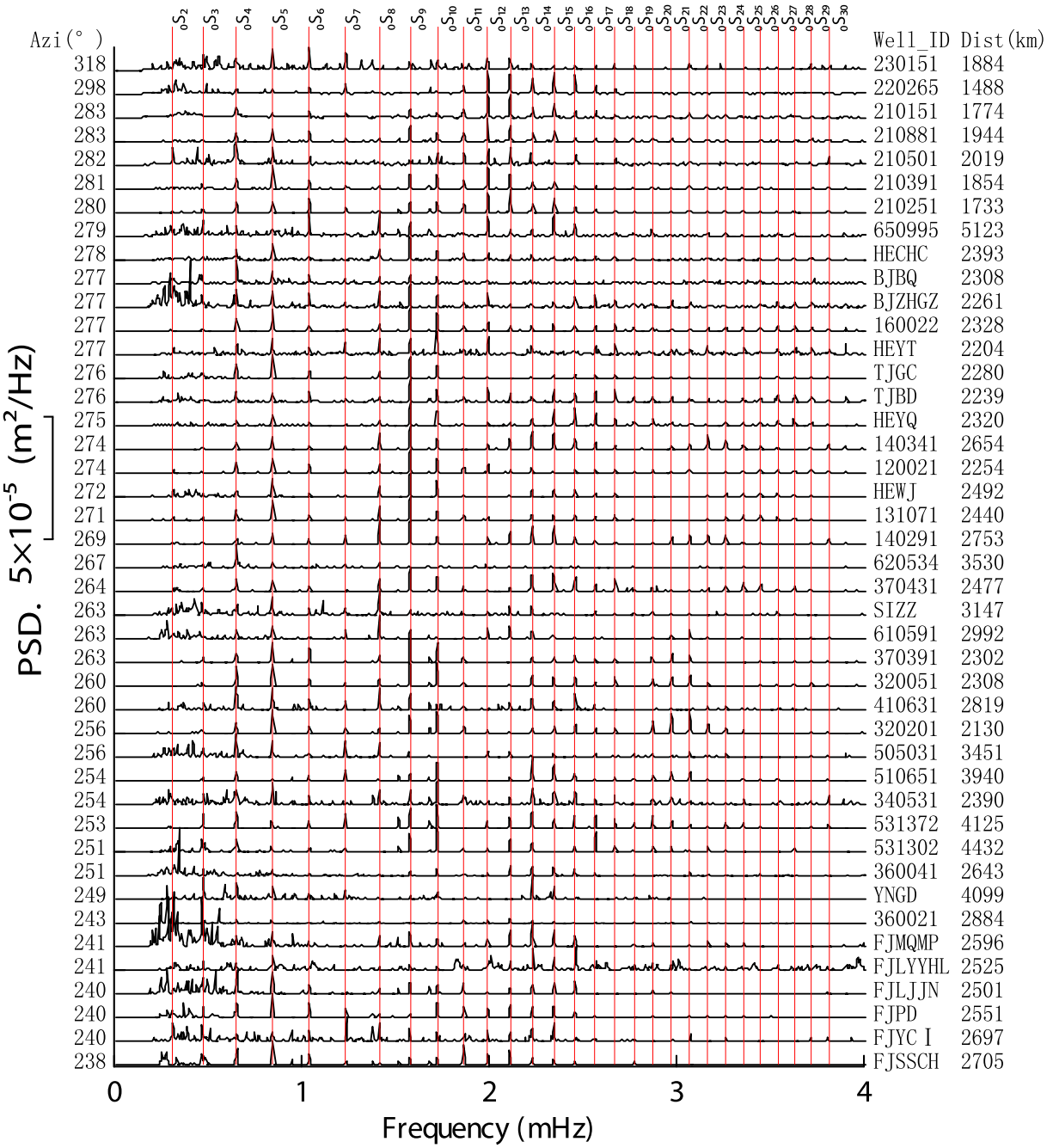

Figure 3. Power spectral density (normalized to amplitude of unity) of water level oscillations at 43 well sites within 220 hr after the M_w 9 Tohoku earthquake, sorted by azimuth from the seismic source to the station. The vertical lines correspond to the eigenfrequencies of the Earth's free oscillations. ${}_0S_l$ indicates the spheroidal modes of the Earth's free oscillations. For clarity, the amplitudes were normalized to the maximum amplitude of the power spectrum density. Well IDs and well-epicentre distances are listed on the right side of each curve.

amplitudes of the tidal constituents were calculated with Baytap-G (Ishiguro & Tamura 1985), the calculating error was given as Root Mean Square Error (RMSE). For further details the reader is referred to Yan *et al.* (2014).

At 85 out of 216 well sites, maximum amplitude water level oscillations up to 3 m were recorded during the passage of the seismic waves (Yan *et al.* 2014). From these 85 wells, we selected 43 sites for this study (Fig. 1), which are characterized as follows: (i) continuous oscillations for several hours after the occurrence of the earthquake, (ii) high sensitivity to earthquake shaking and solid earth tides characterized by the lowest RMSE among the 216 wells and (iii) availability of basic information about the monitoring wells.

The epicentral distances of the selected wells range from 1488 to 5123 km, while the azimuths range from 238° to 318°. The oscillatory response to seismic waves could be observed at these well sites after the occurrence of the earthquake, recording the gravest spheroidal modes of the Earth's free oscillations, and the successive passages of surface waves circling the globe several times after the earthquake. The amplitudes of the water level oscillations at different sites varied greatly. The maximum amplitude during the passage of the first surface wave was 3 m, with a mean value of

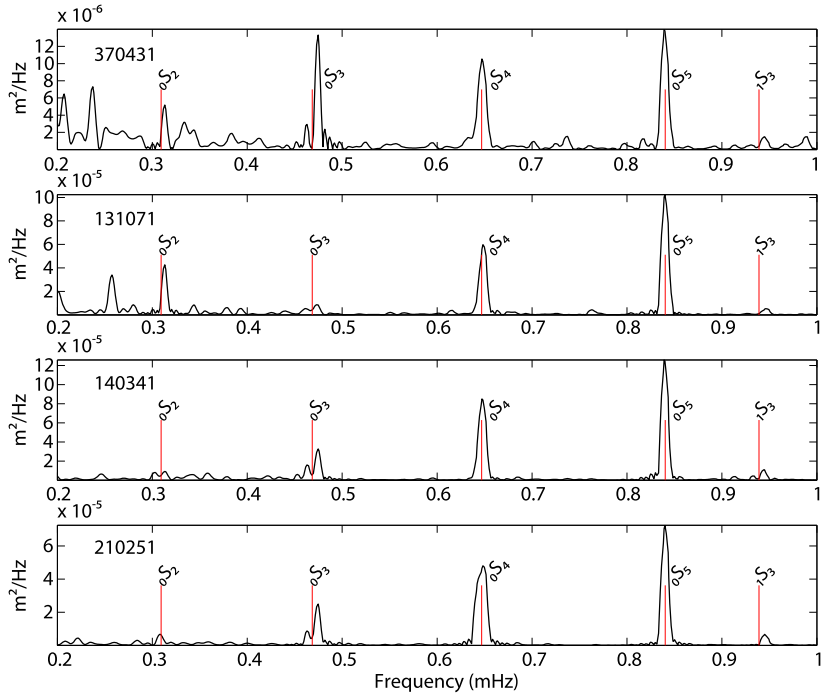

Figure 4. Power spectral density of water level oscillations at four quiet well sites.

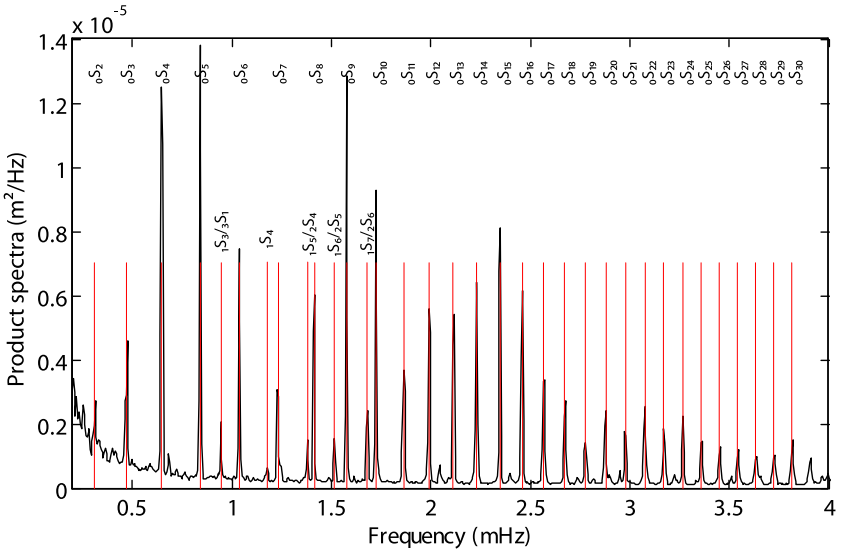

Figure 5. Product spectrum from the 43 considered wells.

0.35 m. During the passage of the earth-circling waves the amplitudes ranged from several millimetres to tens of centimetres. Time series of the well water level at each site are shown in Fig. 2. Well IDs are the same as in Yan *et al.* (2014), where the reader can find additional information about the well-aquifer systems as well as the tidal admittance of each well.

3 FREQUENCY ESTIMATION METHODS

There are numerous frequency estimation methods for detecting modes of the Earth's free oscillations, most of which have roots in conventional Fourier harmonic analysis, while some are non-Fourier-based spectral methods (Chao & Gilbert 1980; Thomson 1982; Masters & Gilbert 1983; Roult & Clévédé 2000; Carlin & Louis 2008; Rosat *et al.* 2008; Ding & Shen 2013; Shen & Ding 2014).

Considering periodic, exponentially decaying harmonic signals that exist in a noisy time series, Chao & Gilbert (1980) devised a method, referred to as the AR method, to estimate the complex frequencies. This method is robust in estimating the complex frequency and amplitude of harmonic signals in noisy time series, and has been successfully used to estimate the frequencies and quality factors of the Earth's normal modes recorded in long-period seismograms and superconducting gravimeter (Chao & Gilbert 1980; Masters & Gilbert 1983; Chao *et al.* 1990; Ding & Shen 2014; Ding & Chao 2015). In this study, we use the AR method to analyse the well water level data. Because the details of the estimation method have been introduced in Chao & Gilbert (1980), we will not repeat them here and refer the reader to that work.

Due to the fact that the SNRs of the various well water level records for the 2011 Tohoku M_w 9.0 earthquake are different, some multiplets of a mode may appear in one record, but not appear in others. As scaling differences induced by different well-aquifer systems exist, the AR method is used to estimate the singlets of one target mode from each record separately. Thereafter, we use the geometrical mean of all estimates as the final estimation, the product spectrum, that is $[\prod_n P_n(\omega)]^{1/N}$, where N is the number of records used (Smylie *et al*. 1993). The product spectrum reduces the noise variance by the factor N all across the spectrum and increases the modal SNRs. Furthermore, since the logarithm of $[\prod_n P_n(\omega)]^{1/N}$ is equal to $\frac{1}{N}\sum_n \log P_n(\omega)$, any scaling difference induced by different well-aquifer systems among the component spectra only introduces static offsets and hence does not matter in practice (Ding & Chao 2015).

Before frequency estimation, tidal effects were removed in all 43 wells as in the previous paper (Yan *et al*. 2014). For 27 wells with barometric records, the local barometric effects were corrected (Zürn & Widmer 1995; Zürn & Wielandt 2007; Zürn *et al*. 2007). The barometric admittance ranges from 0.9 to 16.5 mm hPa^{-1}, with a mean of 7.3 mm hPa^{-1} and a median of 6.7 mm hPa^{-1}. The M_2 tidal factors range from 0.9 to 18.2 GPa, with a mean of 6.9 GPa, and a median of 5.7 GPa. The barometric admittances are positively correlated with tidal factors. For the other 16 wells, due to a lack of barometric data, we could not correct for barometric effects in our calculation. A test revealed that there was no obvious difference in the product spectra whether the barometric pressure effect had been corrected or not. A Hann window was used to improve the robustness of estimation by reducing spectral leakages (Harris 1978; Chao & Gilbert 1980).

4 RESULTS AND DISCUSSION

4.1 Detection of Earth's free oscillations

In order to compare the normal modes of the free oscillations among different well sites, the AR spectral density analysis was applied to each well water level record. 220 hr of data were used as a record after the earthquake, and a Hann window was multiplied with the data before the spectral analysis. Fig. 3 clearly shows that all 43 wells contain distinguishable spectral peaks between the frequencies of 1–4 mHz. Note that all spectral peaks match spheroidal fundamental mode frequencies. Incidentally, every peak is related to a fundamental mode multiplet (each multiplet actually contains $2l+1$ singlets, where l is the angular degree). At some quiet well sites, the long-period fundamental modes are clearly legible, for example, at sites 210251, 140341, 131071 and 370431, both ${}_0S_2$ and ${}_0S_3$ modes can be identified in the single spectra (Fig. 4). However, not all of the singlets of ${}_0S_2$ (see examples from superconducting gravimeter recordings in Häfner & Widmer-Schnidrig 2013) are detected at these stations.

As depicted in Fig. 3, not all of the modes were detectable at each well. Especially at lower frequencies, some of the wells showed higher noise levels. In order to improve the SNRs, we calculated the product spectrum (Fig. 5). The product spectrum reduces the noise variance by a factor of 43 all across the spectrum and reduces scaling differences induced by different well-aquifer systems among the component spectra. Fig. 5 shows that the modes of the free oscillations can be clearly detected, which match well with the fundamental spheroidal modes, ${}_0S_l$ ($l = 2$–31). In addition, some spikes are significantly higher than the background noise in the product spectrum, coinciding with overtones of the spheroidal modes, such as, ${}_1S_3/{}_3S_1$, ${}_1S_4$, ${}_1S_5/{}_2S_4$, ${}_1S_6/{}_2S_5$ and ${}_1S_7/{}_2S_6$.

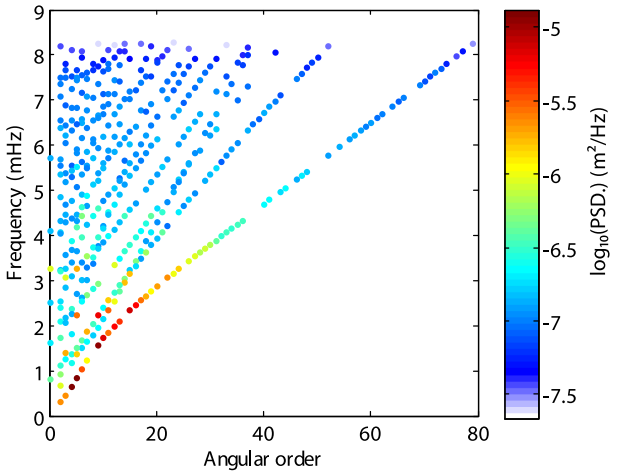

Figure 6. Dispersion diagram for 494 spheroidal modes (with periods >2 min) of the PREM model. Shown are free-oscillation frequencies detected from the 43 wells as a function of the harmonic degree.

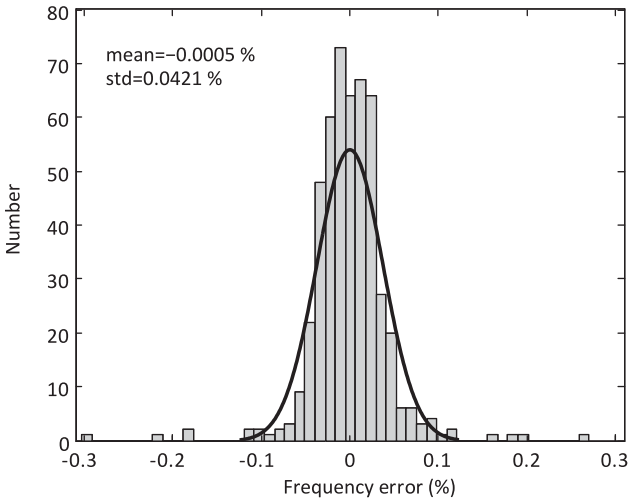

Figure 7. Histogram of the frequency resolution error of different modes detected from 43 well records.

The eigenfrequencies of the oscillations detected from the product spectrum of 43 groundwater wells are shown in Fig. 6 as a function of angular degree for the spheroidal modes, with the colour scale indicating the logarithm of the detected amplitude. The redder the colour is, the more reliable the detected frequency can be assigned. Furthermore, not only fundamental modes, but also some overtones can be detected by these well water level oscillations. The detected frequencies are mainly below 5 mHz, and the angular degrees are mainly below 40.

In order to check the frequency-resolution error of different modes corresponding to theoretical frequencies, the differences between the detected frequency values from the product spectrum of 43 well sites and the frequency values based on the Preliminary Reference Earth Model (PREM; Dziewonski & Anderson 1981) were calculated. 494 modes shown in Fig. 6 were tested. The frequency-resolution error is defined as the ratio of the frequency differences to the frequency values of the PREM. Fig. 7 shows the distribution of the frequency-resolution error from the product spectrum of 43 well records. As the theoretical frequencies of Earth's free

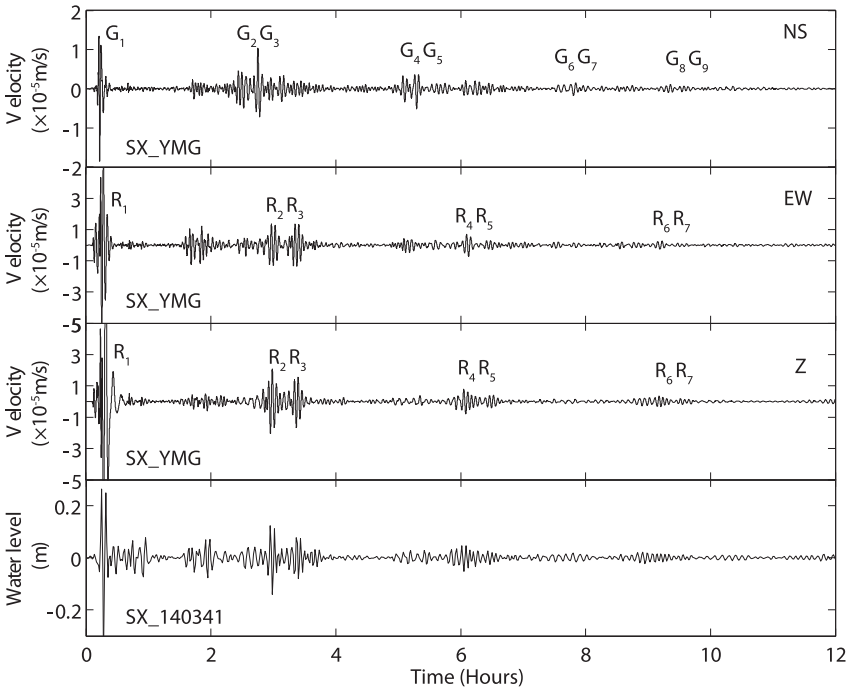

Figure 8. Globe-circling Rayleigh (R) and Love (G) surface waves recorded at the three-component broad-band seismic station YMG and the well water level site 140341 over 12 hr after the Tohoku M_w 9 earthquake. The seismograms have been corrected for instrument response by deconvolution. Both seismograms and water level records were filtered by a Butterworth bandpass filter from 2 to 5 mHz.

oscillation modes are directly related to the geophysical parameters of the PREM, the small frequency-resolution errors (one standard deviations is about 0.04 per cent) indicate that well water level data may provide some valuable information about the Earth's deep structure, which will help to improve upon existing earth models.

4.2 Comparison between groundwater level and broad-band seismograms

In order to reveal the essential characteristics of the well water level response to seismic waves, we compared the water level oscillations with broadband seismic records, both in the time and frequency domains. Fig. 8 is an example of the comparison of water level records (site 140341, see Fig. 1) with three-component velocity records from a broadband seismometer located at site YMG, in the immediate vicinity of the well (about 27 km) over a period of 12 hr after the Tohoku M_w 9.0 earthquake. Instrument responses (BBVS 60 s 50 Hz) have been corrected by deconvolution of seismograms. A Butterworth bandpass filter between 2 and 5 mHz was applied to both data sets. Globe-circling Rayleigh waves were visible up to the R7 in both the seismograms and water level records. However, globe-circling Love waves up to G8 or even G9 were visible only in the seismograms, but not in the water level records because no (or negligible) volume change can be caused by the Love waves.

In order to study the normal modes of the Earth's free oscillation, amplitude spectra of the records from both water level and broad-band seismograms were calculated and compared. The frequencies of normal modes were calculated with PREM and the fundamental modes are indicated by thin vertical lines in Fig. 9. There are some differences in the amplitude spectra between water level and seismograms. In the higher frequency range, both seismograms and water level records have a high SNR except for the transversal component of the seismogram. The transversal component seems strange with a single, strong line at ${}_0T_{12}$. One reason for the pronounced line might be that ${}_0T_{12}$ is strongly coupled to ${}_0S_{11}$ via the Coriolis force (Zürn *et al*. 2000). However, at this site, in the lower frequency range (frequency smaller than 1.5 mHz), a significant increase of the seismic noise inhibits the study of the gravest free oscillations. Contrary, the water level data have the highest SNR in the lower frequency range, especially below 1.5 mHz.

The water level data show spectral peaks associated with the spheroidal modes of the gravest free oscillations. For instance, the fundamental spheroidal modes ${}_0S_3$, ${}_0S_4$, ${}_0S_5$, ${}_0S_6$ and ${}_0S_7$ are clearly visible in water level records, but undistinguishable in seismograms. Apart from the fundamental modes, many small amplitude modes can be distinguished in the water level records. In our case, the comparison analysis of amplitude spectra between water level and broadband seismograms (BBVS 60 s 50 Hz) illustrates the higher quality of water level data at very low frequencies, which is very significant for the study of the gravest free oscillations. It should be noted, however, that this statement cannot be generalized. The example was selected to demonstrate how sensitive groundwater systems can be.

4.3 Earth's background free oscillations

Ocean infragravity waves in the shallow and deep oceans or atmospheric turbulence acting on the Earth's surface can also excite free oscillations of the Earth, termed the Earth's Background Free Oscillations (Suda *et al*. 1998; Nawa *et al*. 2000; Fukao *et al*. 2002; Nishida 2013). In order to check for the background free oscillations, power spectral densities (PSDs) of water level were calculated for a time interval of three months before and after the Tohoku M_w 9 earthquake. Fig. 10 is an example from well site 140341 showing that the PSD is significantly lower before the earthquake than

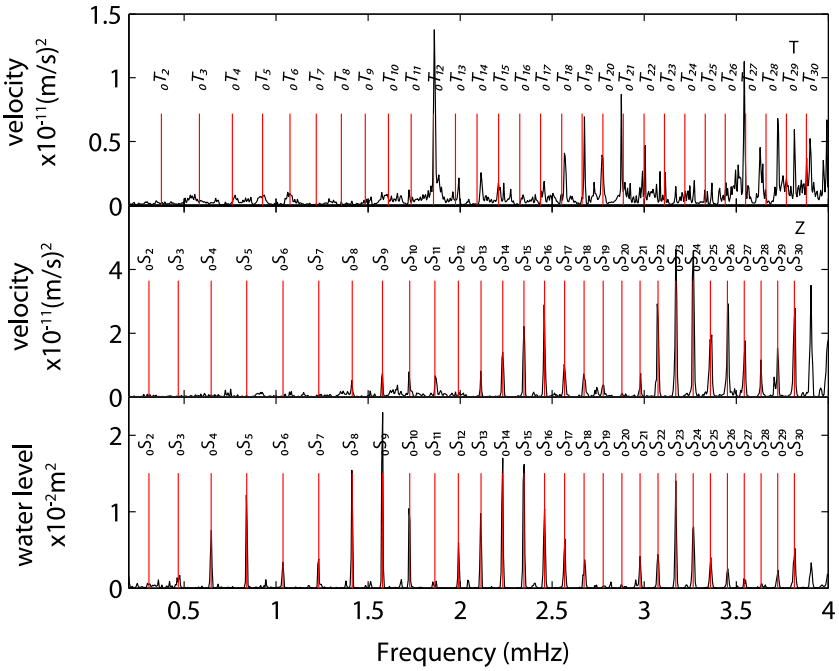

Figure 9. Comparison between the amplitude spectra of the seismograms after the Tohoku M_w 9 earthquake recorded at seismic station YMG and the water level at site 140341 (both records are 220 hr long). Vertical lines indicate the eigenfrequencies of the fundamental toroidal or spheroidal modes for the PREM. Instrument response had been conducted by deconvolution on the seismograms.

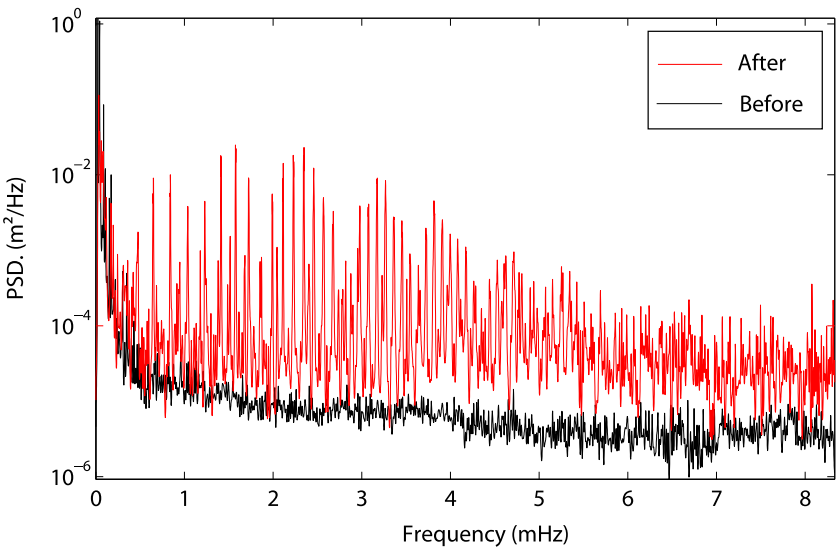

Figure 10. Comparison of power spectral densities (PSDs) before and after the Tohoku M_w 9 earthquake at well site 140341. The black and red curves indicate the PSDs before and after the earthquake, respectively.

after it, which means that the free oscillations were caused by the earthquake rather than ocean infra-gravity waves.

5 CONCLUSIONS AND OUTLOOK

Earth's free oscillation phenomena provide an independent tool to investigate the Earth's interior structure. For the first time—to the best of our knowledge—the Earth's free oscillations induced by a mega-thrust earthquake were resolved within an array of 43 groundwater wells. Records from single wells provide solid evidence for groundwater level responses to the modes of the Earth's free oscillations. After the occurrence of the earthquake, globe circling Rayleigh surface waves were recorded up to the R7. It has been revealed that the principal oscillatory fluctuations seen in the well water level records correspond to spheroidal modes ${}_0S_l$ ($l = 2$–31 for frequencies between 0.3 and 5 mHz) of free oscillation. Although the background noise of some wells precludes the study of the gravest modes, the product spectra method can efficiently improve the SNRs even at very low (<1.5 mHz) frequencies.

Broad-band seismometers, superconducting gravimeters, ring lasers, tiltmeters, strainmeters, laser extensometers, and recently, also differential GPS observations have been used to detect free oscillation signals. These technologies have good SNRs in their

corresponding frequency bands. However, such instrumentation requires major efforts in terms of investment as well as maintenance, and thus the spatial availability of the data is limited on a global scale. On the contrary, water level data are easily available, with monitoring sites relatively well distributed globally. Approximately 42 000 long-term observation wells exist in the United States that have 5 or more years of water level records (Taylor & Alley 2001). Assuming that only 1‰ of these wells are sensitive to Earth tides, a few tens of wells might have the potential to detect Earth's free oscillations in the United States alone. Globally, we may crudely estimate a virtual array of sensitive water wells of the order of some hundred sites. Furthermore, water level data may have high sensitivities at very low frequency signals, and it might be advantageous to sample strain at depth (hundreds of metres to kilometres) instead of measuring strain at the surface. Thus, groundwater level data should be considered as a low-cost complementary tool to study the Earth's free oscillations and, subsequently, better improve our models of the Earth's interior.

Due to the long-periodic nature of the Earth's free oscillations, the site-specific aquifer response to these long-periodic excitations may provide further insight into the local hydrogeological conditions in future studies—in a similar way as the response to Earth tides can be used (Elkhoury *et al*. 2006) to infer temporal variations of the aquifer properties deduced from changes in amplitude and phase of the tidal components. To this end, it might be worthwhile to investigate the feasibility to use seismic source functions to predict the anticipated strain response in each of the wells and to cross-correlate it with the particular modes seen at each well site. Furthermore, it needs to be addressed why the fundamental radial mode ${}_0S_0$—which is normally expected—was not detected in the well water level records.

ACKNOWLEDGEMENTS

We are grateful to Walter Zürn (BFO) and an anonymous reviewer for constructive, critical and encouraging comments and suggestions to improve our manuscript. We thank Xiufen Zheng of Institute of Geophysics, CEA, for providing the seismic wave data. Many thanks to Torsten Dahm (GFZ) for fruitful discussions and comments, and to Kevin Fleming (GFZ) for improving our English. This work is supported by the National Natural Science Foundation of China (41503114).

REFERENCES

Alsop, L.E., Sutton, G.H. & Ewing, M., 1961. Free oscillations of the Earth observed on strain and pendulum seismographs, *J. geophys. Res.,* **66,** 631–641.

Benioff, H., 1958. Long waves observed in the Kamchatka earthquake of November 4, 1952, *J. geophys. Res.,* **63,** 589–593.

Benioff, H., Harrison, J.C., LaCoste, L., Munk, W.H. & Slichter, L.B., 1959. Searching for the Earth's Free Oscillations, *J. geophys. Res.,* **64,** 1334–1337.

Benioff, H., Press, F. & Smith, S., 1961. Excitation of the Free Oscillations of the Earth by Earthquakes, *J. geophys. Res.,* **66,** 605–619.

Beroza, G.C. & Jordan, T.H., 1990. Searching for slow and silent earthquakes using free oscillations, *J. geophys. Res.,* **95,** 2485–2510.

Bodvarsson, G., 1970. Confined fluids as strain meters, *J. geophys. Res.,* **75,** 2711–2718.

Bogiatzis, P. & Ishii, M., 2014. Constraints on the moment tensor of the 2011 Tohoku-Oki Earthquake from Earth's free oscillations, *Bull. seism. Soc. Am.,* **104,** 875–884.

Brodsky, E.E., Roeloffs, E., Woodcock, D., Gall, I. & Manga, M., 2003. A mechanism for sustained groundwater pressure changes induced by distant earthquakes, *J. geophys. Res.,* **108,** 2390, doi:10.1029/2002JB002321.

Carlin, B.P. & Louis, T.A., 2008. *Bayesian Methods for Data Analysis,* 3rd edn, CRC Press, 552 pp.

Chao, B.F., 1990. Comment on "A new method of spectral analysis and its application to the Earth's free oscillations: the 'Sompi' Method" by S. Hori *et al*., *J. geophys. Res.,* **95,** 19 789–19 790.

Chao, B.F. & Gilbert, F., 1980. Autoregressive estimation of complex eigenfrequencies in low frequency seismic spectra, *Geophys. J. Int.,* **63,** 641–657.

Cooper, H.H., Bredehoeft, J.D., Papadopulos, I.S. & Bennett, R.R., 1965. The response of well-aquifer systems to seismic waves, *J. geophys. Res.,* **70,** 3915–3926.

Derr, J.S., 1969. Internal structure of the Earth inferred from free oscillations, *J. geophys. Res.,* **74,** 5202–5220.

Deuss, A., Ritsema, J. & van Heijst, H., 2011. Splitting function measurements for Earth's longest period normal modes using recent large earthquakes, *Geophys. Res. Lett.,* **38,** L046115, doi:10.1029/2010gl046115.

Ding, H. & Chao, B.F., 2015. Detecting harmonic signals in a noisy time-series: the z-domain Autoregressive (AR-z) spectrum, *Geophys. J. Int.,* **201,** 1287–1296.

Ding, H. & Shen, W.B., 2013. Search for the Slichter modes based on a new method: optimal sequence estimation, *J. geophys. Res.,* **118,** 5018–5029.

Ding, H. & Shen, W.-B., 2014. Determination of the complex frequencies for the normal modes below 1 mHz after the 2010 Maule and 2011 Tohoku earthquakes, *Ann. Geophys.,* **56,** S0563, doi:10.4401/ag-6400.

Dziewonski, A.M. & Anderson, D.L., 1981. Preliminary reference Earth model, *Phys. Earth planet. Inter.,* **25,** 297–356

Dziewonski, A.M. & Gilbert, F., 1972. Observations of normal modes from 84 recordings of the Alaskan Earthquake of 1964 March 28, *Geophys. J. R. astr. Soc.,* **27,** 393–446.

Eaton, J.P. & Takasaki, K.J., 1959. Seismological interpretation of earthquake-induced water-level fluctuations in wells, *Bull. seism. Soc. Am.,* **49,** 227–245.

Elkhoury, J.E., Brodsky, E.E. & Agnew, D.C., 2006. Seismic waves increase permeability, *Nature,* **441,** 1135–1138.

Ferreira, A.M.G., d'Oreye, N.F., Woodhouse, J.H. & Zürn, W., 2006. Comparison of fluid tiltmeter data with long-period seismograms: surface waves and Earth's free oscillations, *J. geophys. Res.,* **111,** B11307, doi:10.1029/2006JB004311.

Fukao, Y., Nishida, K., Suda, N., Nawa, K. & Kobayashi, N., 2002. A theory of the Earth's background free oscillations, *J. geophys. Res.,* **107,** ESE 11-1–ESE 11-10.

Häfner, R. & Widmer-Schnidrig, R., 2013. Signature of 3-D density structure in spectra of the spheroidal free oscillation ${}_0S_2$, *Geophys. J. Int.,* **192,** 285–294.

Harris, F.J., 1978. On the use of windows for harmonic analysis with the discrete Fourier transform, *Proc. IEEE,* **66,** 51–83.

Hwang, R.-D., 2014. First-order rupture features of the 2011 M_w 9.0 Tohoku (Japan) earthquake from surface waves, *J. Asian Earth Sci.,* **81,** 20–27.

Ide, S., Baltay, A. & Beroza, G.C., 2011. Shallow dynamic overshoot and energetic deep rupture in the 2011 M_w 9.0 Tohoku-Oki Earthquake, *Science,* **332,** 1426–1429.

Igel, H., Nader, M.-F., Kurrle, D., Ferreira, A.M.G., Wassermann, J. & Schreiber, K.U., 2011. Observations of Earth's toroidal free oscillations with a rotation sensor: the 2011 magnitude 9.0 Tohoku-Oki earthquake, *Geophys. Res. Lett.,* **38,** L21303, doi:10.1029/2011GL049045.

Ishiguro, M. & Tamura, Y., 1985. BAYTAP-G in TIMSAC-84, *Comput. Sci. Monogr.,* **22,** 56–117.

Kanamori, H. & Anderson, D.L., 1975. Amplitude of the Earth's free oscillations and long-period characteristics of the earthquake source, *J. geophys. Res.,* **80,** 1075–1078.

Kawabe, I., Ohno, I. & Nadano, S., 1988. Groundwater flow records indicating earthquake occurrence and induced Earth's free oscillations, *Geophys. Res. Lett.,* **15,** 1235–1238.

Kubo, H. & Kakehi, Y., 2013. Source process of the 2011 Tohoku Earthquake estimated from the joint inversion of teleseismic body waves and geodetic data including seafloor observation data: source model with enhanced reliability by using objectively determined inversion settings, *Bull. seism. Soc. Am.,* **103,** 1195–1220.

Lambotte, S., Rivera, L. & Hinderer, J., 2007. Constraining the overall kinematics of the 2004 Sumatra and the 2005 Nias Earthquakes using the Earth's gravest free oscillations, *Bull. seism. Soc. Am.,* **97,** S128–S138.

Laske, G. & Masters, G., 1999. Limits on differential rotation of the inner core from an analysis of the Earth's free oscillations, *Nature,* **402,** 66–69.

Liu, L.-B., Roeloffs, E. & Zheng, X.-Y., 1989. Seismically induced water level fluctuations in the WaIi Well, Beijing, China, *J. geophys. Res.,* **94,** 9453–9462.

Masters, G. & Gilbert, F., 1983. Attenuation in the earth at low frequencies, *Phil. Trans. R. Soc. A,* **308,** 479–522.

Mitsui, Y. & Heki, K., 2012. Observation of Earth's free oscillation by dense GPS array: after the 2011 Tohoku megathrust earthquake, *Sci. Rep.,* **2,** doi:10.1038/srep00931.

Molodenskii, S.M., 2010. Correctives to the scheme of the Earth's structure inferred from new data on nutation, tides, and free oscillations, *Izv. Phys. Solid Earth,* **46,** 555–579.

Molodenskii, S.M. & Molodenskaya, M.S., 2009. On mechanical Q parameters of the lower mantle inferred from data on the Earth's free oscillations and nutation, *Izv. Phys. Solid Earth,* **45,** 744–752.

Nader, M.F., Igel, H., Ferreira, A.M.G., Kurrle, D., Wassermann, J. & Schreiber, K.U., 2012. Toroidal free oscillations of the Earth observed by a ring laser system: a comparative study, *J. Seismol.,* **16,** 745–755.

Nawa, K. *et al.*, 2000. Incessant excitation of the Earth's free oscillations: global comparison of superconducting gravimeter records, *Phys. Earth planet. Inter.,* **120,** 289–297.

Ness, N.F., Harrison, J.C. & Slichter, L.B., 1961. Observations of the free oscillations of the Earth, *J. geophys. Res.,* **66,** 621–629.

Nishida, K., 2013. Earth's background free oscillations, *Annu. Rev. Earth planet. Sci.,* **41,** 719–740.

Okal, E.A. & Stein, S., 2009. Observations of ultra-long period normal modes from the 2004 Sumatra-Andaman earthquake, *Phys. Earth planet. Inter.,* **175,** 53–62.

Park, J. *et al.*, 2005. Earth's free oscillations excited by the 26 December 2004 Sumatra-Andaman Earthquake, *Science,* **308,** 1139–1144.

Park, J., Amoruso, A., Crescentini, L. & Boschi, E., 2008. Long-period toroidal earth free oscillations from the great Sumatra–Andaman earthquake observed by paired laser extensometers in Gran Sasso, Italy, *Geophys. J. Int.,* **173,** 887–905.

Ren, J., Chen, H., Jiang, C.U., Wang, S., Wen, C., Yang, Y. & Wang, C., 2009. Earth's free spheroidal oscillations of the Great Sumatra Earthquake observed with digital water level meter, *J. Seismol. Res.,* **32,** 333–338.

Rexin, E.E., Oliver, J. & Prentiss, D., 1962. Seismically-induced fluctuations of the water level in the Nunn-Bush well in Milwaukee, *Bull. seism. Soc. Am.,* **52,** 17–25.

Rosat, S., Fukushima, T., Sato, T. & Tamura, Y., 2008. Application of a non-linear damped harmonic analysis method to the normal modes of the Earth, *J. Geodyn.,* **45,** 63–71.

Roult, G. & Clévédé, E., 2000. New refinements in attenuation measurements from free-oscillation and surface-wave observations, *Phys. Earth planet. Inter.,* **121,** 1–37.

Shen, W.-B. & Ding, H., 2014. Observation of spheroidal normal mode multiplets below 1 mHz using ensemble empirical mode decomposition, *Geophys. J. Int.,* **196,** 1631–1642.

Smylie, D.E., Hinderer, J., Richter, B. & Ducarme, B., 1993. The product spectra of gravity and barometric pressure in Europe, *Phys. Earth planet. Inter.,* **80,** 135–157.

Suda, N., Nawa, K. & Fukao, Y., 1998. Earth's background free oscillations, *Science,* **279,** 2089–2091.

Suzuki, W., Aoi, S., Sekiguchi, H. & Kunugi, T., 2011. Rupture process of the 2011 Tohoku-Oki mega-thrust earthquake (*M*9.0) inverted from strong-motion data, *Geophys. Res. Lett.,* **38,** L00G16, doi:10.1029/2011GL049136.

Taylor, C.J. & Alley, W.M., 2001. Ground-water-level monitoring and the importance of long-term water-level data, in *U.S. Geological Survey Circular 1217,* Reston, Virginia, 68 p.

Thomson, D.J., 1982. Spectrum estimation and harmonic analysis, *Proc. IEEE,* **70,** 1055–1096.

Woodhouse, J.H. & Deuss, A., 2007. Theory and observations - Earth's free oscillations, in *Treatise on Geophysics*, pp. 31–65, ed. Schubert, G., Elsevier.

Yan, R., Woith, H. & Wang, R., 2014. Groundwater level changes induced by the 2011 Tohoku earthquake in China mainland, *Geophys. J. Int.,* **199,** 533–548.

Zürn, W. & Widmer, R., 1995. On noise reduction in vertical seismic records below 2 mHz using local barometric pressure, *Geophys. Res. Lett.,* **22,** 3537–3540.

Zürn, W. & Wielandt, E., 2007. On the minimum of vertical seismic noise near 3 mHz, *Geophys. J. Int.,* **168,** 647–658.

Zürn, W., Laske, G., Widmer-Schnidrig, R. & Gilbert, F., 2000. Observation of Coriolis coupled modes below 1 mHz, *Geophys. J. Int.,* **143,** 113–118.

Zürn, W., Exß, J., Steffen, H., Kroner, C., Jahr, T. & Westerhaus, M., 2007. On reduction of long-period horizontal seismic noise using local barometric pressure, *Geophys. J. Int.,* **171,** 780–796.

Zürn, W., Ferreira, A.M.G., Widmer-Schnidrig, R., Lentas, K., Rivera, L. & Clévédé, E., 2015. High-quality lowest-frequency normal mode strain observations at the Black Forest Observatory (SW-Germany) and comparison with horizontal broad-band seismometer data and synthetics, *Geophys. J. Int.,* **203,** 1786–1803.